Transmission Line Parameter Error Identification and Estimation in Three-Phase Networks

Ramtin Khalili, *Student Member, IEEE*, and Ali Abur, *Fellow, IEEE*

***Abstract*—This paper concerns the detection and identification of errors in the parameters of three-phase transposed as well as untransposed transmission line (TL) models used by various network applications. Such detailed models are increasingly needed in particular by power system applications where loads may not be balanced and/or TLs may not be symmetrical, and a full detailed three-phase solution may have to be obtained. To address this problem, the paper proposes an efficient algorithm for detection, identification, and estimation of parameter errors using synchronized phasor measurements. The suspect TL is detected using the modal domain networks in the first stage. The developed algorithm extends the previously developed largest normalized Lagrange multiplier (NLM) test for positive sequence parameters to the full coupled three-phase lines. An estimation method is also proposed for estimating the erroneous parameters, which takes into account the correlation of the parameters. To illustrate the effectiveness of the method, several tests are performed on the IEEE 118-bus system and a large 3474-bus utility system.**

***Index Terms*—Parameter error identification, modal component transformation, synchronized phasor measurements, three-phase networks.**

I. Introduction

INCREASED penetration of renewable energy sources and demand-side management practices in power systems necessitate closer monitoring of the system states. To this end, state estimation (SE) algorithms implemented in the energy management systems (EMS) are of importance. While traditionally positive sequence models and associated analyses have been used, unbalanced injections by unconventional sources and loads necessitate three-phase SE implementation. SE formulation using the three-phase network model is presented in [1] accounting for the phase imbalances in the transmission and distribution systems. Comparing the results of three-phase and positive sequence SE on different case studies revealed that the SE error is significant when using the positive sequence equivalent [1]. Furthermore, another common approximation used in the positive sequence models, namely the assumption of fully transposed transmission lines, can be relaxed in the three-phase formulation. However, in order to reach an unbiased SE solution, accurate parameters of the TLs should be known. Also, other crucial applications such as optimal relay settings [2]–[3], accurate fault location, and dynamic simulations all rely heavily on TL parameters.

Phasor measurement units (PMUs) provide global positioning satellite (GPS) synchronized voltage and current phasor measurements at a high sampling rate [4]. The use of PMU measurements which are linear functions of the system states, enables a non-iterative solution of the SE problem. Thus, convergence problems which may be encountered using conventional measurements are avoided. Numerous research papers elaborated on PMU-based SE and its improvements in [5]–[7]. A three-phase linear tracking SE is described in [8] that is developed as part of of a Virginia Electric and Power Company project [9]. Valuable experiences with the PMU-based three-phase SE at Dominion Energy over the past ten years are described in [10].

An efficient approach for three-phase SE has been developed based on the modal decomposition method described in [11]. The key novelty of this approach is based on the linearity of equations that allows the modal decomposition of the measurements into three independent measurement sets in each mode and subsequent superposition of the modal components of the SEs in order to recover the three-phase states. The limitation of the proposed method in [11] is that the network model should be symmetrical. Recently, this assumption is relaxed in [12] by extending the method to more general power systems with untransposed TLs.

Database errors related to network model parameters exist for various reasons. These include aging, changes in ambient temperature, unreported conductor reconfiguration or type, as well as manual database entry errors. These errors can bias the SE solution and cause the bad data processing function to incorrectly identify and remove certain *valid* measurements as incorrect that further exacerbate the solution. Furthermore, since the database is shared by multiple applications, their performance will be directly affected. The issue of parameter error detection and estimation using PMUs has been the subject of various investigations in the past. Parameter estimation has been performed using multiple measurement scans in [13] and [14] to increase the measurement redundancy. The total least squares concept has been utilized for parameter estimation in [15]. Also, it has been demonstrated in [15] that this method has a lower estimation error in comparison with the ordinary least squares. Parameter estimation in the presence of systematic voltage and current measurement error has been investigated in [16] and [17]. Nonetheless, all these methods are

Manuscript received April 11, 2021; revised August 23, 2021; accepted October 3, 2021. Date of publication October 11, 2021; date of current version April 19, 2022. This work made use of ERC shared facilities supported by the ERC Program of the NSF and the DOE under NSF Award Number EEC-1041877. Paper no. TPWRS-00571-2021. *(Corresponding author: Ali Abur.)*

The authors are with the ECE Department, Northeastern University, Boston, MA 02135 USA (e-mail: khalili.r@husky.neu.edu; abur@ece.neu.edu).

Color versions of one or more figures in this article are available at https://doi.org/10.1109/TPWRS.2021.3118007.

Digital Object Identifier 10.1109/TPWRS.2021.3118007

based on the positive sequence equivalent. Parameter estimation for three-phase networks with untransposed TLs has also been discussed in [18]–[21]. An ordinary least squares approach is used in [18], and a robust M-estimator is proposed in [19] in order to mitigate the impact of bad data and outliers on the parameter estimation. The authors in [20] argued that estimation based on the transmittance matrix model is less sensitive to the measurement noise. However, the shunt elements are neglected in this study. Both studies [19], [20] consider an isolated single transmission line measured at both ends unlike this paper which can handle any line parameter using wide-area measurements without requiring a PMU at every bus. Combined transmission line parameter estimation and measurement calibration using PMU data has been suggested in [22]. Furthermore, approaches based on three-phase parameter estimation using a dynamic state and parameter estimator [23] and traveling waves [24] are also proposed.

The parameter estimation references above are within the scope of simultaneous state and parameter estimation methods. The other broad category encompasses sequential methods based on the SE results. In this approach, first one or more parameter(s) is (are) flagged as suspect parameter(s) and then the correct parameter(s) is (are) estimated. Early approaches in this category are based on analyzing the sensitivity of measurement residuals to parameter errors as discussed in [25]–[27]. Although they are simple to implement, their reliability is limited. Later on, other approaches that assume a suspect set of parameters and estimate them along with the system states using an augmented state vector are proposed in [28]–[30]. Since it is difficult to predict the suspect set, its size may grow rapidly, making these approaches impractical for the large-scale systems. Finally, a reliable method based on the normalized Lagrange multiplier (NLM) test is proposed and then further improved in [31] for positive sequence networks. This method is shown to be computationally efficient and statistically robust even when measurement and parameter errors occur simultaneously. As demonstrated in [32], [33], PMU measurements at strategic locations can enhance the performance of the NLM method for identifying erroneous parameters.

This paper proposes and develops an efficient three-stage algorithm to identify the parameter errors and estimate the correct values in three-phase systems using PMU measurements. The proposed method is capable of detecting and estimating errors in the self and mutual branch parameters for untransposed as well as transposed TLs. The preliminary results of the paper, including only the detection of the erroneous branch for transposed TLs, are presented in [34]. The most important contributions of the present paper can be summarized as follows: 1) Development of a new algorithm, where the suspect branch is identified using the modal domain NLM method for untransposed as well as transposed TLs, and then the erroneous parameters are identified and estimated by formulating the three-phase extension of the NLM test for the local network adjacent to the suspect line. This method simplifies the analysis and avoids building of coupled three-phase measurement jacobian with respect to states as well as all the self and mutual coupling parameters of the whole network. 2) Given the strong correlation between the parameters of a three-phase TL which makes the estimation process cumbersome, a novel parameter estimation approach is formulated based on the residuals and the covariance matrix of the Lagrange multipliers to simultaneously estimate all of the parameters of the suspect TL. 3) Formulation and solution of a PMU placement approach to ensure parameter error identification for all system branches in a three-phase system fully observed by PMUs. Note that the methods described in [14]–[24] lack any measurement placement strategy and require PMUs installed at both ends of the TL, while the developed PMU placement strategy does not have such requirements, and is capable of identifying errors by placing fewer PMUs. A comparison of the key features of this paper and several relevant references is provided in Table I.

TABLE I
COMPARISON BETWEEN THE PROPOSED METHOD AND LITERATURE

	[13]	[18]	[19]	[20]	[23]	[24]	[34]	This paper
Three-phase TL		■	■	■	■	■	■	■
Untransposed TL		■	■	■	■			■
Does not need PMUs at both ends	■						■	■
Measurement Placement Strategy								■
Scalability study			■					■
Hierarchical parameter error detection/estimation	■							■
Use of modal domain analysis		■				■	■	■

II. THREE-PHASE STATE ESTIMATION USING SYNCHRONIZED PHASOR MEASUREMENTS

A. Decoupled SE Fromulation

It has been shown that if the network is fully observable by PMUs and if the measurements and states are considered in the rectangular coordinates (rather than polar coordinates), the following measurement model will hold true:

$$\boldsymbol{Z} = \boldsymbol{H} \,.\, \boldsymbol{V} + \boldsymbol{e} \tag{1}$$

where:

$\boldsymbol{Z}$	$3m \times 1$ three-phase PMU measurement vector
$\boldsymbol{H}$	$3m \times 3n$ three-phase measurement jacobian
$\boldsymbol{V}$	$3n \times 1$ three-phase state vector
$\boldsymbol{e}$	$3m \times 1$ three-phase measurement error vector
n	Number of states (irrespective of number of phases)
m	Number of measurements (irrespective of number of phases)

In this paper, boldface variables denote a matrix or a vector. In the above equation all the voltage and current phasors are considered in the rectangular coordinates. So, the measurement vector is given by (2) shown at the bottom of the next page, where $\phi = \{a, b, c\}$. Also, $\mathscr{R}$ and $\mathscr{I}$ denote the real and imaginary parts of the corresponding variable, respectively. It has been shown in [11] that the following transformation matrix $\boldsymbol{T}$ can transform

phase domain variables into the modal (sequence) domain:

$$\boldsymbol{T} = \frac{1}{3}\begin{bmatrix} 1 & 1 & 1 \\ 1 & \alpha & \alpha^2 \\ 1 & \alpha^2 & \alpha \end{bmatrix}, \quad \alpha = e^{j(\frac{2\pi}{3})} \tag{3}$$

By applying the block diagonal form of $\boldsymbol{T}$ to (1), the three-phase SE problem is transformed into the following form in the modal domain:

$$\begin{bmatrix} \mathbf{Z}^0 \\ \mathbf{Z}^+ \\ \mathbf{Z}^- \end{bmatrix} = \begin{bmatrix} \mathbf{H}^0 & \mathbf{H}^{0+} & \mathbf{H}^{0-} \\ \mathbf{H}^{+0} & \mathbf{H}^{+} & \mathbf{H}^{+-} \\ \mathbf{H}^{-0} & \mathbf{H}^{-+} & \mathbf{H}^{-} \end{bmatrix} \begin{bmatrix} \mathbf{V}^0 \\ \mathbf{V}^+ \\ \mathbf{V}^- \end{bmatrix} + \begin{bmatrix} \mathbf{e}^0 \\ \mathbf{e}^+ \\ \mathbf{e}^- \end{bmatrix} \tag{4}$$

where, "0," "+," and "−" superscripts, represent the associated variable or matrix in the *zero*, *positive*, and *negative* sequence, respectively. If the network is three-phase symmetrical, mutual impact of modes will be zero and (4) can be expressed as three independent single-phase SE problems as follows:

$$\begin{cases} \boldsymbol{Z}^0 = \boldsymbol{H}^0 \,.\, \boldsymbol{V}^0 + \boldsymbol{e}^0 \\ \boldsymbol{Z}^+ = \boldsymbol{H}^+ \,.\, \boldsymbol{V}^+ + \boldsymbol{e}^+ \\ \boldsymbol{Z}^- = \boldsymbol{H}^- \,.\, \boldsymbol{V}^- + \boldsymbol{e}^- \end{cases} \tag{5}$$

For the sake of brevity, in the sequel 0, +, and − sequence matrices and vectors will be indicated by a superscript $s = \{0, +, -\}$. The estimated state $\hat{\boldsymbol{V}}^s$ for the "s" mode obtained using three decoupled measurement equations given by (5) can be written as:

$$\hat{\boldsymbol{V}}^s = [\boldsymbol{G}^s]^{-1}[\boldsymbol{H}^s]^T \boldsymbol{W}^s \boldsymbol{Z}^s \tag{6}$$

where $\boldsymbol{W}$ is the weight matrix defined as the inverse of measurement error covariance matrix ($\boldsymbol{R}$). Also, $\boldsymbol{G}^s$ represents the gain matrix for SE problems related to each mode. Modal domain gain matrices and measurement residuals are defined as:

$$\boldsymbol{G}^s = [\boldsymbol{H}^s]^T \boldsymbol{W}^s \boldsymbol{H}^s \tag{7}$$

$$\boldsymbol{r}^s = \boldsymbol{Z}^s - \boldsymbol{H}^s \hat{\boldsymbol{V}}^s \tag{8}$$

Bad data can be identified using the largest normalized residuals (LNR) test as described in [11].

B. Modeling Three-Phase Transmission Lines

In general the three-phase branch impedance matrix for the branch connecting bus k to m is represented by a 3×3 impedance/admittance matrix. For the reason that will be illustrated in the next part, representing the three-phase TL by its admittance matrix is more helpful. Furthermore, admittance representation can also help to express series and shunt admittances separately as follows:

$$Y_{km}^{abc} = \begin{bmatrix} y_{km}^{aa} & y_{km}^{ab} & y_{km}^{ac} \\ y_{km}^{ab} & y_{km}^{bb} & y_{km}^{bc} \\ y_{km}^{ac} & y_{km}^{bc} & y_{km}^{cc} \end{bmatrix}$$

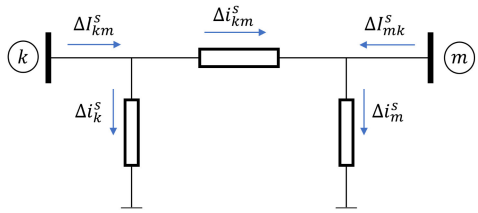

Fig. 1. Π-equivalent of Transmission Line: Compensation Notation.

$$Y_{sh,k}^{abc} = \begin{bmatrix} y_{sh,k}^{aa} & y_{sh,k}^{ab} & y_{sh,k}^{ac} \\ y_{sh,k}^{ab} & y_{sh,k}^{bb} & y_{sh,k}^{bc} \\ y_{sh,k}^{ac} & y_{sh,k}^{bc} & y_{sh,k}^{cc} \end{bmatrix} \tag{9}$$

where, superscript *abc* denotes that the impedance is in the *phase* or *abc* domain. Applying $\boldsymbol{T}(Y_{km}^{abc})\boldsymbol{T}^{-1}$ and $\boldsymbol{T}(Y_{sh,k}^{abc})\boldsymbol{T}^{-1}$ yield the modal domain counterparts for the series and shunt admittances:

$$Y_{km}^{seq} = \begin{bmatrix} y_{km}^{00} & y_{km}^{0+} & y_{km}^{0-} \\ y_{km}^{+0} & y_{km}^{++} & y_{km}^{+-} \\ y_{km}^{-0} & y_{km}^{-+} & y_{km}^{--} \end{bmatrix}$$

$$Y_{sh,k}^{seq} = \begin{bmatrix} y_{sh,k}^{00} & y_{sh,k}^{0+} & y_{sh,k}^{0-} \\ y_{sh,k}^{+0} & y_{sh,k}^{++} & y_{sh,k}^{+-} \\ y_{sh,k}^{-0} & y_{sh,k}^{-+} & y_{sh,k}^{--} \end{bmatrix} \tag{10}$$

For fully transposed TLs, the off-diagonal entries in (10) are zero. However, in the case of untransposed TL, the off-diagonal elements should be taken into account.

C. Decoupled SE for Unsymmetrical Networks

As mentioned in subSection II-A, (4) and (5) will be identical if and only if the network is completely symmetrical. However, if the TLs are untransposed, the off-diagonal elements of (4) are not zero and three-phase measurement model cannot be decoupled into three single-phase subsystems. A practical yet effective approach where the decoupled SE formulation can be generalized to networks including untransposed TLs by incorporating a compensation method is recently developed in [12].

Fig. 1 demonstrates the Pi-equivalent of the TL $k - m$, where the current compensation terms due to the off-diagonal entries indicated by Δ. Δi_{km} denotes the series component; Δi_k and Δi_m denote the shunt components of the current compensation at both ends. According to the off-diagonal entries of Y_{km}^{seq} in (10), the series components of the compensation term are derived as follows:

$$\begin{cases} \Delta i_{km}^0 = y^{0+}(V_k^+ - V_m^+) + y^{0-}(V_k^- - V_m^-) \\ \Delta i_{km}^+ = y^{+0}(V_k^0 - V_m^0) + y^{+-}(V_k^- - V_m^-) \\ \Delta i_{km}^- = y^{-0}(V_k^0 - V_m^0) + y^{-+}(V_k^+ - V_m^+) \end{cases} \tag{11}$$

$$\boldsymbol{Z}^T = \left[\mathscr{R}\{V^\phi\} \mid \mathscr{I}\{V^\phi\} \mid \mathscr{R}\{I_i^\phi\} \mid \mathscr{I}\{I_i^\phi\} \mid \mathscr{R}\{I_{ij}^\phi\} \mid \mathscr{I}\{I_{ij}^\phi\}\right] \tag{2}$$

By substituting $y = g + jb$ for the mutual admittances in (11), the rectangular coordinate counterparts for the series component can be obtained as follows:

$$\begin{aligned}\mathscr{R}\{\Delta i^0_{km}\} = {} & g^{0+}(\mathscr{R}\{V^+_k\} - \mathscr{R}\{V^+_m\}) \\ & - b^{0+}(\mathscr{I}\{V^+_k\} - \mathscr{I}\{V^+_m\}) \\ & + g^{0-}(\mathscr{R}\{V^-_k\} - \mathscr{R}\{V^-_m\}) \\ & - b^{0-}(\mathscr{I}\{V^-_k\} - \mathscr{I}\{V^-_m\}) \qquad (12)\end{aligned}$$

$$\begin{aligned}\mathscr{I}\{\Delta i^0_{km}\} = {} & g^{0+}(\mathscr{I}\{V^+_k\} - \mathscr{I}\{V^+_m\}) \\ & + b^{0+}(\mathscr{R}\{V^+_k\} - \mathscr{R}\{V^+_m\}) \\ & + g^{0-}(\mathscr{I}\{V^-_k\} - \mathscr{I}\{V^-_m\}) \\ & + b^{0-}(\mathscr{R}\{V^-_k\} - \mathscr{R}\{V^-_m\}) \qquad (13)\end{aligned}$$

$\mathscr{R}\{\Delta i^+_{km}\}$, $\mathscr{I}\{\Delta i^+_{km}\}$, $\mathscr{R}\{\Delta i^-_{km}\}$, and $\mathscr{I}\{\Delta i^-_{km}\}$ are also derived for the "+" and "−" modes. Similarly, the shunt component of the current compensation are determined considering the off-diagonal entries of $Y^{seq}_{sh,k}$ in (10):

$$\begin{cases}\Delta i^0_k = y^{0+}_{sh,k}(V^+_k) + y^{0-}_{sh,k}(V^-_k) \\ \Delta i^+_k = y^{+0}_{sh,k}(V^0_k) + y^{+-}_{sh,k}(V^-_k) \\ \Delta i^-_k = y^{-0}_{sh,k}(V^0_k) + y^{-+}_{sh,k}(V^+_k)\end{cases} \qquad (14)$$

by substituting $y_{sh} = g_{sh} + jb_{sh}$ in (14), the rectangular coordinate values are obtained:

$$\begin{aligned}\mathscr{R}\{\Delta i^0_k\} = {} & g^{0+}_{sh}(\mathscr{R}\{V^+_k\}) - b^{0+}_{sh}(\mathscr{I}\{V^+_k\}) \\ & + g^{0-}_{sh}(\mathscr{R}\{V^-_k\}) - b^{0-}_{sh}(\mathscr{I}\{V^-_k\}) \qquad (15)\end{aligned}$$

$$\begin{aligned}\mathscr{I}\{\Delta i^0_k\} = {} & g^{0+}_{sh}(\mathscr{I}\{V^+_k\}) + b^{0+}_{sh}(\mathscr{R}\{V^+_k\}) \\ & + g^{0-}_{sh}(\mathscr{I}\{V^-_k\}) + b^{0-}_{sh}(\mathscr{R}\{V^-_k\}) \qquad (16)\end{aligned}$$

$\mathscr{R}\{\Delta i^+_k\}$, $\mathscr{I}\{\Delta i^+_k\}$, $\mathscr{R}\{\Delta i^-_k\}$, $\mathscr{I}\{\Delta i^-_k\}$, at bus k; $\mathscr{R}\{\Delta i^0_m\}$, $\mathscr{I}\{\Delta i^0_m\}$, $\mathscr{R}\{\Delta i^+_m\}$, $\mathscr{I}\{\Delta i^+_m,\}$, $\mathscr{R}\{\Delta i^-_m\}$, and $\mathscr{I}\{\Delta i^-_m\}$ at bus m are determined in a similar way.

As shown in Fig. 1 for the untransposed TL $k-m$, the current compensation terms in both directions are given by:

$$\begin{cases}\Delta I^s_{km} = \Delta i^s_{km} + \Delta i^s_k \\ \Delta I^s_{mk} = -\Delta i^s_{km} + \Delta i^s_m\end{cases} \qquad (17)$$

current compensations (17) are rewritten in the rectangular coordinates as the standard form of measurements defined in (2):

$$\begin{cases}\mathscr{R}\{\Delta I^s_{km}\} = \mathscr{R}\{\Delta i^s_{km}\} + \mathscr{R}\{\Delta i^s_k\} \\ \mathscr{I}\{\Delta I^s_{km}\} = \mathscr{I}\{\Delta i^s_{km}\} + \mathscr{I}\{\Delta i^s_k\}\end{cases} \qquad (18)$$

$$\begin{cases}\mathscr{R}\{\Delta I^s_{mk}\} = -\mathscr{R}\{\Delta i^s_{km}\} + \mathscr{R}\{\Delta i^s_m\} \\ \mathscr{I}\{\Delta I^s_{mk}\} = -\mathscr{I}\{\Delta i^s_{km}\} + \mathscr{I}\{\Delta i^s_m\}\end{cases} \qquad (19)$$

The compensation terms defined in (18) and (19) are equivalent measurements reflecting the impact of the off-diagonal terms. In other words, instead of using the non-decoupled form of (4), the decoupled form of (5) can still be utilized by adding the current compensation terms to the modal domain measurements.

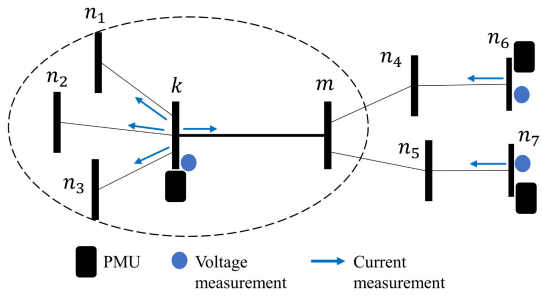

Fig. 2. Observable PMU Configuration No. 1.

Since the currents defined in (11) and (14) are related to the states in different modes, the solution will be recursive. First, the off-diagonal terms will be neglected in order to initialize the SE algorithm. In each iteration compensation terms will be updated based on the SE results in the previous iteration. Then, measurements will be updated and states are re-estimated using (6)–(7) until reaching to the termination criterion. Note that although the proposed decoupled SE is recursive, it will not impose a huge computational burden on the algorithm because $\boldsymbol{H}^s$, $\boldsymbol{G}^s$, and $\boldsymbol{W}^s$ remain constant unless there is a change in network parameters or topology.

III. PMU Placement Approach

A systematic PMU placement algorithm is developed to ensure parameter estimation and error identification of all TLs in the system. Optimal PMU placement (OPP) problem is commonly formulated for state observability as an integer linear programming (ILP) problem given by [35]:

$$\begin{aligned}& Minimize \sum_{i=1}^{n_b} c_i x_i \\ & s.t. \quad \boldsymbol{A}.\boldsymbol{X} \geq \boldsymbol{1} \qquad (20)\end{aligned}$$

where, $\boldsymbol{A}$ is the *binary bus connectivity matrix*. Considering $\mathcal{N}_i$ as the set of all the adjacent buses to bus i, $\boldsymbol{A}$ is defined as follows:

$$\boldsymbol{A}_{ij} = \begin{cases}1 & \text{if} \quad i = j \quad or \quad j \in \mathcal{N}_i \\ 0 & \text{otherwise}\end{cases} \qquad (21)$$

the rest of the variables in (20) are defined as follows:

n_b	Number of buses
c_i	PMU installation cost at bus i
x_i	binary PMU decision variable at bus i (1: PMU bus, 0: non-PMU bus)
$\boldsymbol{X}$	$n_b \times 1$ vector of PMU decision variables

The constraint $\boldsymbol{A}.\boldsymbol{X} \geq \boldsymbol{1}$ implies that each bus should be observed by PMUs at least one time. An observable PMU configuration is shown in Fig. 2 where the line $k-m$ is the suspect TL. While Fig. 2 and the OPP in (20) ensure full PMU observability and hence the state estimation feasibility, it will not guarantee successful parameter error identification due to a low redundancy. There are three necessary conditions for enabling parameter error identification and estimation for the proposed

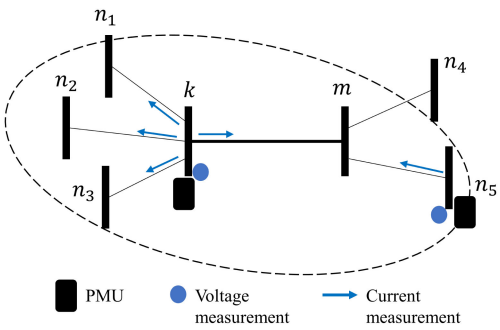

Fig. 3. Observable PMU Configuration No. 2.

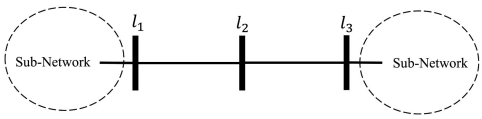

Fig. 4. Radial Transmission Lines Structure.

method. In order to formulate a PMU Placement problem, only the constraint in the original OPP (20) should be modified.

(a) First, a PMU should be placed at one end of the suspect TL in order to observe the parameters of the line (for instance bus k in Fig. 2). So, this constraint can be written as follows:

$$\boldsymbol{U}.\boldsymbol{X} \geq \mathbf{1} \tag{22}$$

where, $\boldsymbol{U}$ is the *branch to bus incidence matrix* defined as follows:

$$\boldsymbol{U}_{ij} = \begin{cases} 1 & \text{if } j\text{is From/To bus of the } i^{\text{th}} \text{ branch} \\ 0 & \text{otherwise} \end{cases} \tag{23}$$

Transformer branches are excluded from $\boldsymbol{U}$ since there is no need to have a PMU at one end of a transformer.

(b) Apart from the PMU at bus k, the other end of the line should also be observed indirectly by another PMU in its neighboring buses. This configuration is demonstrated in Fig. 3. In other words, non-PMU buses should be observed at least two times by PMUs installed at $\mathcal{N}_m$. So, $\boldsymbol{A}.\boldsymbol{X} \geq \mathbf{1}$ will be changed to $\boldsymbol{A}.\boldsymbol{X} \geq \mathbf{2}$ for the non-PMU buses. Therefore, the constraint for both the PMU and non-PMU buses can be expressed as $\boldsymbol{A}.\boldsymbol{X} \geq \mathbf{2} - \boldsymbol{X}$ and further summarized as follows:

$$(\boldsymbol{A} + \boldsymbol{I})\,.\,\boldsymbol{X} \geq \mathbf{2} \tag{24}$$

where, $\boldsymbol{I}$ is an $n_b \times n_b$ identity matrix.

(c) It has been shown in [33] that parameter errors in radial structures needs more PMUs to be detectable. For instance, for identifying the parameter error in the lines $l_1 - l_2$ and $l_2 - l_3$ in Fig. 4, a PMU should be installed at the common bus, i.e., bus l_2. Determining these structures is straightforward using the $\boldsymbol{A}$ matrix. The number of non-zero elements in the row/column corresponding to bus l_2 is exactly three. Therefore, the constraint would be $\{x_i = 1 : i \in \mathcal{R}_{rd}\}$ where $\mathcal{R}_{rd}$ is the set of buses in the radial structures.

Thus, considering the constraints in (a), (b), and (c), the PMU placement approach that guarantees the parameter error identification can be formulated as follows:

$$Minimize \sum_{i=1}^{n_b} c_i x_i$$

$$s.t. \quad \begin{cases} (a) : \boldsymbol{U}.\boldsymbol{X} \geq \mathbf{1} \\ (b) : (\boldsymbol{A} + \boldsymbol{I}).\boldsymbol{X} \geq \mathbf{2} \\ (c) : \{x_i = 1 : i \in \mathcal{R}_{rd}\} \end{cases} \tag{25}$$

Note that if there are already-installed PMUs, they can easily be taken into account by adding extra equality constraints to (25). Also, channel limits on PMUs which are not considered in this study can be readily incorporated as described in [36].

IV. Parameter Error Identification and Estimation Algorithm

The proposed parameter error detection and estimation approach is explained in what follows through three different stages in subsetions A-C. Generally, this method is concerned with first detecting the suspect TL based on the modal decomposition applied to the three-phase network, identifying the erroneous parameter using the three-phase NLM test, and then estimating the true value based on the three-phase SE solution of a local sub-network. This method is implemented in a recursive form where in each iteration parameters of the suspect TL are identified and the algorithm is repeatedly executed.

A. Detecting the Suspect Transmission Line

The first stage involves identification of the three-phase TL whose parameters are suspected to be erroneous. This is accomplished by using the previously developed decoupled three-phase SE method where the WLS SE is solved directly for each mode using (6) and (7). The decoupled formulation that is modified to handle untransposed TLs, which is reviewed in subSection II-C is employed at this stage. Once the SE solution is obtained, erroneous parameters should be detected. This step requires the use of the jacobian with respect to the modal domain parameters ($\boldsymbol{H}_p$). The current flow through the line $k - m$ can be expressed as follows:

$$I_{km} = (V_k - V_m)Y_{km} + jY_{sh,k}V_k \tag{26}$$

where, Y_{km} and $Y_{sh,k}$ are the series admittance and line charging susceptance of the TL $k - m$. By substituting $Y_{km} = g_{km} + jb_{km}$ and $Y_{sh,k} = jb_{sh}$, real and imaginary parts of I_{km} can be separated as follows:

$$\begin{aligned} \mathscr{R}\{I_{km}\} &= g_{km}(\mathscr{R}\{V_k\} - \mathscr{R}\{V_m\}) \\ &\quad - b_{km}(\mathscr{I}\{V_k\} - \mathscr{I}\{V_m\}) - b_{sh}\,\mathscr{I}\{V_k\} \end{aligned} \tag{27}$$

$$\begin{aligned} \mathscr{I}\{I_{km}\} &= g_{km}(\mathscr{I}\{V_k\} - \mathscr{I}\{V_m\}) \\ &\quad + b_{km}(\mathscr{R}\{V_k\} - \mathscr{R}\{V_m\}) + b_{sh}\,\mathscr{R}\{V_k\} \end{aligned} \tag{28}$$

Considering the measurement structure of (2) in the modal domain, $\boldsymbol{H}_p$ can be formed as follows:

$$\boldsymbol{H}_p = \begin{array}{c} \\ \partial\mathscr{R}\{V_i\} \\ \partial\mathscr{I}\{V_i\} \\ \partial\mathscr{R}\{I_{ij}\} \\ \partial\mathscr{I}\{I_{ij}\} \end{array} \begin{array}{c} \begin{array}{ccc} \partial\boldsymbol{R} & \partial\boldsymbol{X} & \partial\boldsymbol{b} \end{array} \\ \left[\begin{array}{c|c|c} 0 & 0 & 0 \\ 0 & 0 & 0 \\ \hline [*] & [*] & [*] \\ [*] & [*] & [*] \end{array}\right] \end{array} \tag{29}$$

where:

i, j	$i, j = 1, \ldots, k, m, \ldots, n_b$
$\boldsymbol{R}$	$[r_{ij}]$: $1 \times n_l$ vector of branch resistance
$\boldsymbol{X}$	$[x_{ij}]$: $1 \times n_l$ vector of branch reactance
$\boldsymbol{b}$	$[b_{ij}]$: $1 \times n_l$ vector of branch susceptance
n_l	No. of branches (irrespective of no. of phases)

Note that although current injections are also used they are not shown in the matrices due to the similarity of their derivation and space limitations. As evident from (29), the derivative of current measurement with respect to the parameters which are shown with $[*]$ should be calculated. Considering $i = k$ and $j = m$ and (27)–(28), the partial derivatives for I_{km} and the associated parameters can be obtained using the chain rule as follows:

$$\begin{aligned} &\left[\begin{array}{c|c|c} \frac{\partial\mathscr{R}\{I_{km}\}}{\partial r_{km}} & \frac{\partial\mathscr{R}\{I_{km}\}}{\partial x_{km}} & \frac{\partial\mathscr{R}\{I_{km}\}}{\partial b_{sh,k}} \\ \hline \frac{\partial\mathscr{I}\{I_{km}\}}{\partial r_{km}} & \frac{\partial\mathscr{I}\{I_{km}\}}{\partial x_{km}} & \frac{\partial\mathscr{I}\{I_{km}\}}{\partial b_{sh,k}} \end{array}\right] \\ &= \left[\begin{array}{c|c|c} \mathscr{R}\{V_k\} - \mathscr{R}\{V_m\} & \mathscr{I}\{V_k\} - \mathscr{I}\{V_m\} & -\mathscr{I}\{V_k\} \\ \hline \mathscr{I}\{V_k\} - \mathscr{I}\{V_m\} & \mathscr{R}\{V_k\} - \mathscr{R}\{V_m\} & \mathscr{R}\{V_k\} \end{array}\right] \\ &\quad \times \left[\begin{array}{c|c|c} \frac{\partial g_{km}}{\partial r_{km}} & \frac{\partial g_{km}}{\partial x_{km}} & 0 \\ \frac{\partial b_{km}}{\partial r_{km}} & \frac{\partial b_{km}}{\partial x_{km}} & 0 \\ \hline 0 & 0 & 1 \end{array}\right] \end{aligned} \tag{30}$$

where,

$$\left[\begin{array}{cc} \frac{\partial g_{km}}{\partial r_{km}} & \frac{\partial g_{km}}{\partial x_{km}} \\ \frac{\partial b_{km}}{\partial r_{km}} & \frac{\partial b_{km}}{\partial x_{km}} \end{array}\right] = \left[\begin{array}{cc} \frac{x_{km}^2 - r_{km}^2}{(r_{km}^2 + x_{km}^2)^2} & \frac{-2 r_{km} x_{km}}{(r_{km}^2 + x_{km}^2)^2} \\ \frac{2 r_{km} x_{km}}{(r_{km}^2 + x_{km}^2)^2} & \frac{x_{km}^2 - r_{km}^2}{(r_{km}^2 + x_{km}^2)^2} \end{array}\right] \tag{31}$$

By calculating (30) and (31) for all the measurements and parameters in the modal domain, the jacobian of (29) will be built. Note that there are three $\boldsymbol{H}_p$ matrices corresponding to *zero*, *positive*, and *negative* sequence equivalents. Using the $\boldsymbol{H}_p$, the Lagrange multipliers for each mode will be:

$$\boldsymbol{\lambda} = -[\boldsymbol{H}_p]^T \boldsymbol{W} \boldsymbol{r} \tag{32}$$

In order to perform the NLM test, the i^{th} Lagrange multiplier in (32) associated with the i^{th} parameter is normalized against the (i, i) diagonal entry of Lagrange multiplier covariance matrix $\boldsymbol{\Lambda}$ as follows:

$$\boldsymbol{\lambda}_i^N = \frac{\boldsymbol{\lambda}_i}{\sqrt{\boldsymbol{\Lambda}_{ii}}} \tag{33}$$

where, the covariance matrix of the Lagrange multipliers is defined as follows:

$$\boldsymbol{\Lambda} = cov(\boldsymbol{\lambda}) = [\boldsymbol{H}_p]^T \boldsymbol{W} (\boldsymbol{I} - \boldsymbol{K}) \boldsymbol{H}_p \tag{34}$$

$\boldsymbol{K}$ is called hat matrix and it is given by:

$$\boldsymbol{K} = \boldsymbol{H}[\boldsymbol{G}]^{-1}[\boldsymbol{H}]^T \boldsymbol{W} \tag{35}$$

Based on the NLM test, the Lagrange multipliers of (33) are checked against a predetermined threshold which is typically chosen as 3.0. If the largest NLM is greater than 3.0, then the corresponding line and parameter will be flagged as suspect line and erroneous parameter. The $\boldsymbol{H}_p$ which is represented in (29), shows that there are three parameters related to each line (r, x, and b). So, the total number of parameters and hence the NLMs are $3n_l$ (for each mode).

The positive sequence network is the dominant one in comparison with the zero and negative sequences. So, the decision will be made based on the NLM test of the positive sequence network. Hence, performing the NLM test and forming $\boldsymbol{H}_p$ matrices for the zero and negative modes will not be necessary.

It is also worth noting that, although this approach initially identifies a single suspect TL, the algorithm (also the NLM test itself) is actually iterative, where errors are identified and corrected one at a time in each iteration, and the remaining errors will be identified sequentially in subsequent iterations as long as the NLMs remain above the detection threshold.

B. Three-Phase SE and Parameter Error Identification for the Local Sub-Network

Once the suspect TL is detected and the type of the erroneous parameter is determined as explained above, the three-phase parameters of the line will have to be estimated. While this requires a full three-phase SE solution, since the erroneous TL will only impact the adjacent buses, only a small part of the network and measurement set in the electrical vicinity of the suspect TL need to be considered. This simplification will be illustrated next.

First, the three-phase current measurements of (27) and (28) are converted to (36) and (37) as follows:

$$\begin{aligned} \begin{bmatrix} \mathscr{R}\{I_{km}^a\} \\ \mathscr{R}\{I_{km}^b\} \\ \mathscr{R}\{I_{km}^c\} \end{bmatrix} &= \underbrace{\begin{bmatrix} g_{km}^{aa} & g_{km}^{ab} & g_{km}^{ac} \\ g_{km}^{ab} & g_{km}^{bb} & g_{km}^{bc} \\ g_{km}^{ac} & g_{km}^{bc} & g_{km}^{cc} \end{bmatrix}}_{\boldsymbol{G}_{km}} \begin{bmatrix} \mathscr{R}\{V_k^a\} - \mathscr{R}\{V_m^a\} \\ \mathscr{R}\{V_k^b\} - \mathscr{R}\{V_m^b\} \\ \mathscr{R}\{V_k^c\} - \mathscr{R}\{V_m^c\} \end{bmatrix} \\ &\quad - \underbrace{\begin{bmatrix} b_{km}^{aa} & b_{km}^{ab} & b_{km}^{ac} \\ b_{km}^{ab} & b_{km}^{bb} & b_{km}^{bc} \\ b_{km}^{ac} & b_{km}^{bc} & b_{km}^{cc} \end{bmatrix}}_{\boldsymbol{B}_{km}} \begin{bmatrix} \mathscr{I}\{V_k^a\} - \mathscr{I}\{V_m^a\} \\ \mathscr{I}\{V_k^b\} - \mathscr{I}\{V_m^b\} \\ \mathscr{I}\{V_k^c\} - \mathscr{I}\{V_m^c\} \end{bmatrix} \\ &\quad - \underbrace{\begin{bmatrix} b_{s,km}^{aa} & b_{s,km}^{ab} & b_{s,km}^{ac} \\ b_{s,km}^{ab} & b_{s,km}^{bb} & b_{s,km}^{bc} \\ b_{s,km}^{ac} & b_{s,km}^{bc} & b_{s,km}^{cc} \end{bmatrix}}_{\boldsymbol{B}_{s,km}} \begin{bmatrix} \mathscr{I}\{V_k^a\} \\ \mathscr{I}\{V_k^b\} \\ \mathscr{I}\{V_k^c\} \end{bmatrix} \end{aligned} \tag{36}$$

$$\begin{bmatrix}\mathscr{I}\{I_{km}^a\}\\ \mathscr{I}\{I_{km}^b\}\\ \mathscr{I}\{I_{km}^c\}\end{bmatrix} = \underbrace{\begin{bmatrix}g_{km}^{aa} & g_{km}^{ab} & g_{km}^{ac}\\ g_{km}^{ab} & g_{km}^{bb} & g_{km}^{bc}\\ g_{km}^{ac} & g_{km}^{bc} & g_{km}^{cc}\end{bmatrix}}_{\boldsymbol{G}_{km}} \begin{bmatrix}\mathscr{I}\{V_k^a\}-\mathscr{I}\{V_m^a\}\\ \mathscr{I}\{V_k^b\}-\mathscr{I}\{V_m^b\}\\ \mathscr{I}\{V_k^c\}-\mathscr{I}\{V_m^c\}\end{bmatrix}$$
$$+ \underbrace{\begin{bmatrix}b_{km}^{aa} & b_{km}^{ab} & b_{km}^{ac}\\ b_{km}^{ab} & b_{km}^{bb} & b_{km}^{bc}\\ b_{km}^{ac} & b_{km}^{bc} & b_{km}^{cc}\end{bmatrix}}_{\boldsymbol{B}_{km}} \begin{bmatrix}\mathscr{R}\{V_k^a\}-\mathscr{R}\{V_m^a\}\\ \mathscr{R}\{V_k^b\}-\mathscr{R}\{V_m^b\}\\ \mathscr{R}\{V_k^c\}-\mathscr{R}\{V_m^c\}\end{bmatrix}$$
$$+ \underbrace{\begin{bmatrix}b_{s,km}^{aa} & b_{s,km}^{ab} & b_{s,km}^{ac}\\ b_{s,km}^{ab} & b_{s,km}^{bb} & b_{s,km}^{bc}\\ b_{s,km}^{ac} & b_{s,km}^{bc} & b_{s,km}^{cc}\end{bmatrix}}_{\boldsymbol{B}_{s,km}} \begin{bmatrix}\mathscr{R}\{V_k^a\}\\ \mathscr{R}\{V_k^b\}\\ \mathscr{R}\{V_k^c\}\end{bmatrix} \tag{37}$$

where $[\boldsymbol{G}_{km}]$, $[\boldsymbol{B}_{km}]$, and $[\boldsymbol{B}_{s,km}]$ are all 3×3 matrices instead of scalars. Complexity and size of (36) and (37) will be increased drastically in the case of three-phase compared to the single-phase equations. Indeed, this is the main motivation for developing the error detection method in the modal domain in the above subsection. By knowing the suspect TL it is possible to limit the size of matrices by excluding the unnecessary measurements and states from the three-phase formulation. It is shown in [37], that the error due to inaccurate parameters will only have significant impact on the adjacent buses. In order to maintain the robustness of the SE, the suspect TL and one tier out buses on each side will be included in the sub-network. In this reduced local network, only a few measurements and states will be needed to formulate the three-phase SE. Let $\mathcal{N}_i$ be the set of all the adjacent buses to bus i and $\mathcal{N}'_j$ be the adjacent buses to bus j with an installed PMU. Considering TL $k-m$ as the suspect one with a PMU at bus k (for instance configuration of Fig. 3), the local states will be $\mathscr{R}\{V_i^\phi\}$ and $\mathscr{I}\{V_i^\phi\}$ where $i=\{\mathcal{N}_k\cup\mathcal{N}'_m\}$. Also, the local measurements including voltage phasors, current flows, and current injections will be:

voltage: $\{\mathscr{R}\{V_i^\phi\},\mathscr{I}\{V_i^\phi\}\}\quad i=\{\mathcal{N}'_k\cup\mathcal{N}'_m\}$
current-flow: $\{\mathscr{R}\{I_{kj}^\phi\},\mathscr{I}\{I_{kj}^\phi\}\}\quad j=\mathcal{N}_k$
$\{\mathscr{R}\{I_{im}^\phi\},\mathscr{I}\{I_{im}^\phi\}\}\quad i=\mathcal{N}'_m$
current-injection: $\{\mathscr{R}\{I_k^\phi\},\mathscr{I}\{I_k^\phi\}\}$

Sets of current flows and injections will be further enlarged if another PMU is installed at bus m. After solving the three-phase SE, three-phase measurement jacobian with respect to the parameters will be created. According to the admittance in (9) and by considering the symmetry, there will be six parameters associated with each set of $[R_{ij}]$, $[X_{ij}]$, and $[b_{ij}]$:

$$\boldsymbol{p}_{km} = \begin{bmatrix}p_{km}^{aa} & p_{km}^{ab} & p_{km}^{ac}\\ & p_{km}^{bb} & p_{km}^{bc}\\ & & p_{km}^{cc}\end{bmatrix},\quad p=\{R,X,b\} \tag{38}$$

Therefore, there are only six columns associated with six parameters in the local sub-network which is a noticeable reduction in the size of $\boldsymbol{H}_p$ matrix. Corresponding NLMs are calculated using equations similar to (32)–(35) as well. NLMs can be shown in matrix form as follows:

$$\boldsymbol{\lambda}_{km}^N = \begin{bmatrix}\lambda_{aa}^N & \lambda_{ab}^N & \lambda_{ac}^N\\ & \lambda_{bb}^N & \lambda_{bc}^N\\ & & \lambda_{cc}^N\end{bmatrix} \tag{39}$$

Similar to the conventional single-phase NLM test, the parameter corresponding to the largest $\boldsymbol{\lambda}^N$ will indicate the worst parameter error. Due to the high correlation between the parameters in the three-phase TL, all entries in $\boldsymbol{\lambda}^N$ are significant. Note that similar to the single-phase case, chain rule is applied to find the derivatives of measurements with respect to the parameters. These include $[\boldsymbol{G}_{km}]$, $[\boldsymbol{B}_{km}]$, and $[\boldsymbol{B}_{s,km}]$ derivatives with respect to the parameters of (38) which are not explicitly shown here for space limitations.

C. Estimating the Erroneous Parameter

Once the erroneous TL and its parameters are carefully identified, true parameters should be estimated. The measurement model of (1) is based on the perfect network parameters. When the parameters of the network are erroneous, (1) is reformulated as follows:

$$\boldsymbol{Z} = \boldsymbol{H}.\boldsymbol{V} + \boldsymbol{H}_p.\boldsymbol{p}_e + \boldsymbol{e} \tag{40}$$

where, $\boldsymbol{p}_e$ is the parameter error vector. Similarly, the states can be estimated as follows:

$$\hat{\boldsymbol{V}} = [\boldsymbol{G}]^{-1}[\boldsymbol{H}]^T\boldsymbol{W}(\boldsymbol{Z}-\boldsymbol{H}_p.\boldsymbol{p}_e) \tag{41}$$

So, the estimated measurement vector can be derived as:

$$\begin{aligned}\hat{\boldsymbol{Z}} &= \boldsymbol{H}\hat{\boldsymbol{V}} + \boldsymbol{H}_p.\boldsymbol{p}_e\\ &= \boldsymbol{H}([\boldsymbol{G}]^{-1}[\boldsymbol{H}]^T\boldsymbol{W}(\boldsymbol{Z}-\boldsymbol{H}_p.\boldsymbol{p}_e)) + \boldsymbol{H}_p.\boldsymbol{p}_e\\ &= \boldsymbol{K}\boldsymbol{Z} + \boldsymbol{S}\boldsymbol{H}_p.\boldsymbol{p}_e\end{aligned} \tag{42}$$

where, $\boldsymbol{S}=\boldsymbol{I}-\boldsymbol{K}$ is the residual sensitivity matrix. Given the fact that the residual vector is the difference between the measurements and estimated measurements, $\boldsymbol{r}$ can be written as follows:

$$\begin{aligned}\boldsymbol{r} &= \hat{\boldsymbol{Z}}-\boldsymbol{Z} = \boldsymbol{K}\boldsymbol{Z} + \boldsymbol{S}\boldsymbol{H}_p.\boldsymbol{p}_e - \boldsymbol{Z}\\ &= \boldsymbol{S}\boldsymbol{H}_p.\boldsymbol{p}_e - \boldsymbol{S}(\boldsymbol{H}\boldsymbol{V}+\boldsymbol{e}) = \boldsymbol{S}\boldsymbol{H}_p.\boldsymbol{p}_e - \boldsymbol{S}\boldsymbol{e}\end{aligned} \tag{43}$$

considering $E(\boldsymbol{S}\boldsymbol{e})=0$ and $cov(\boldsymbol{S}\boldsymbol{e})=\boldsymbol{S}\boldsymbol{R}$, parameter error $\boldsymbol{p}_e$ can be estimated from (43) as follows:

$$\boldsymbol{p}_e = [\boldsymbol{H}_p^T\boldsymbol{W}(\boldsymbol{I}-\boldsymbol{K})\boldsymbol{H}_p]^{-1}\boldsymbol{H}_p^T\boldsymbol{W}\boldsymbol{r} = \boldsymbol{\Lambda}^{-1}\boldsymbol{H}_p^T\boldsymbol{W}\boldsymbol{r} \tag{44}$$

This vector yields the parameter errors for multiple parameters simultaneously. For most of the cases where parameter error is roughly within a small lower and upper bound of the true value (roughly 10%), one time estimation of (44) yields the desirable results. However, for more stringent cases estimating the true values takes more than one iteration [25], [26]. Since the updated parameter will change the network matrices, $\boldsymbol{H}$ and $\boldsymbol{H}_p$ should be updated in each iteration which is not a burden regarding the local sub-network around the suspect TL which is selected for three-phase SE and parameter estimation.

The main issue with (44) is that $\mathbf{\Lambda}$ is singular when the parameters are highly correlated which is also the case here considering (38). To avoid this problem, knowing the largest NLM from (39), parameters can be reordered in $\boldsymbol{H}_p$ from the most to the least sensitive as follows $\{p_1, p_2, \ldots, p_6\}$. So, (44) can be written as:

$$\begin{pmatrix} \boldsymbol{p}_{e1} \\ \boldsymbol{p}_{e2} \end{pmatrix} = \begin{pmatrix} \mathbf{\Lambda}_1 & \mathbf{\Lambda}_{12} \\ \mathbf{\Lambda}_{12}^T & \mathbf{\Lambda}_2 \end{pmatrix}^{-1} \left(\boldsymbol{H}_{p1} \boldsymbol{H}_{p2} \right)^T \boldsymbol{W} \boldsymbol{r} \tag{45}$$

where only $\boldsymbol{p}_{e1}$ is to be estimated, ignoring p_{e2} which is p_6. Hence, as long as $\mathbf{\Lambda_1}$ is nonsingular $\boldsymbol{p}_{e1}$, which includes p_1 to p_5 can be estimated. $\boldsymbol{H}_p$ and $\boldsymbol{r}$ are then updated and now p_1 is removed from the list of parameters and $\boldsymbol{p}_{e1}$ will yield the estimated error for p_2 to p_6. For instance if parameter X^{bb} has the largest NLM, X^{ac} will be eliminated in the first iteration and X^{aa}, X^{ab}, X^{bb}, X^{bc}, and X^{cc} are estimated. Then, X^{bb} is excluded from the set and other parameters are estimated.

D. Algorithm Summary

Steps of the proposed algorithm can be presented as follows:

Step 1: Determine the selected buses for placing PMUs by solving (25).

Step 2: Compute modal (sequence) components of parameters and measurements. Modal domain admittance matrices can also be formed.

Step 3: Obtain the *zero*, *positive*, and *negative* sequence measurement models of (5) by neglecting the off-diagonal terms and estimate the states using (6) and (7).

Step 4: Calculate the current compensation terms defined in (11)–(19) using the states estimated in the previous iteration and update the measurements associated with the untransposed lines.

Step 5: Re-estimate the states using (6) and (7).

Step 6: *SE termination criterion:* If $|\hat{\boldsymbol{V}}_i - \hat{\boldsymbol{V}}_{i-1}| < \epsilon$, go to the next step otherwise go back to *Step* 4. ϵ is SE threshold which is set as 10^{-6}.

Step 7: Form the measurement jacobian for "0" and "+" modes with respect to the modal parameters (29) based on (30) and (31).

Step 8: Compute the NLMs ((33)–(34)) and NRs in the modal domain.

Step 9: *Error Detection termination criterion:* If the largest NR and/or NLM is greater than the detection threshold of 3.0, then flag the corresponding parameter or measurement as bad, otherwise stop. If bad data is identified, correct the bad data and go back to *Step* 4. In the case of parameter error, the suspect TL is determined; go to the next step.

Step 10: Select the three-phase local sub-network around the suspect TL and estimate the three-phase states.

Step 11: Considering the three-phase measurements and parameters of (38), form the three-phase $\boldsymbol{H}_p$ matrix.

Step 12: Calculate NLMs as (39) corresponding to the 6 suspect parameters using (32)–(35) and declare the largest one as the erroneous parameter. If all $\boldsymbol{\lambda}_{km}^N$ are below 3, there is no error; go back to *Step 2*.

TABLE II
PMU LOCATIONS: IEEE 118-BUS SYSTEM

PMU Buses
{1, 2, 3, 4, 6, 7, 9, 10, 11, 13, 14, 15, 16, 18, 20, 21, 22, 23, 26, 27, 28, 29, 30, 31, 32, 33, 34, 35, 36, 39, 40, 41, 43, 44, 46, 48, 49, 50, 52, 53, 55, 56, 57, 58, 59, 61, 62, 63, 65, 67, 69, 70, 72, 73, 74, 76, 77, 78, 79, 81, 83, 84, 86, 87, 88, 89, 90, 91, 93, 94, 95, 96, 97, 98, 99, 100, 101, 102, 103, 105, 107, 108, 109, 111, 112, 113, 114, 115, 116, 117, 118}

Step 13: Estimate the correct parameters by (45) and go back to *Step* 10.

V. Discussion and Simulation Results

The proposed method is implemented and tested on two modified IEEE 118-bus test systems. In the first modification of the IEEE 118-bus system (*system-I*), loads are intentionally made unbalanced to achieve a voltage unbalance factor (VUF) of 2%. So, the system imbalance in *system-I* is only due to unbalanced loads. Then, in addition to the loads, a transmission line is also made untransposed in the IEEE 118-bus system (*system-II*) in order to test the approach against untransposed TLs. In order to test the scalability of the method, a large high-voltage utility system with 3474 buses and 4644 branches is also studied. Several cases are considered to illustrate the effectiveness of the proposed method in detecting different types of parameter errors. The most common parameter errors are roughly within the range of 10% to 30% of the parameters' true value. Although this is not a limitation for this method, the introduced gross errors in the parameters lie within this range. Unless otherwise stated, PMU locations of Table II that are obtained using the proposed PMU placement approach (Section III), are utilized for all of the test cases.

A. Single Error in a Transmission Line

In this subsection, different types (resistance, reactance, or susceptance) of parameter errors are introduced in only one phase of the TLs. Three cases are simulated using *system-I* where a single parameter error is introduced in each case while assuming no errors in other parameters and measurements:

- *Test A:* r_{15-19}^{aa}, $+30\%$ error, PMU at bus 15.
- *Test B:* x_{41-42}^{cc}, $+30\%$ error, PMU at bus 41.
- *Test C:* $b_{103-110}^{bb}$, $+30\%$ error, PMU at bus 103.

For all these tests, there is only one PMU at one end of the TL. Parameter error detection and estimation results for *tests A*, *B*, and *C* are given in Table III. The maximum values of NR and NLM for the *zero* and *positive* sequence are shown in the first row of Table III. Since parameter errors will impact the measurement residuals, the LNR test results are also reported. The positive sequence NLM in all tests are the largest determining the suspect TL and the parameter. The erroneous TL and the error type which are identified at this stage based on the NLM and LNR test results in the modal domain are presented in the second row of Table III.

TABLE III
IDENTIFICATION, AND ESTIMATION OF A SINGLE PARAMETER ERROR (IEEE 118-BUS SYSTEM)

	Test A	***Test B***	***Test C***
$\boldsymbol{r}^{N0}$ $\boldsymbol{r}^{N+}$	10.44 27.9	20.9 103.2	18.8 14.1
$\boldsymbol{\lambda}^{N0}$ $\boldsymbol{\lambda}^{N+}$	12.57 **34.85**	34.75 **127.43**	17.9 **19.67**
suspect TL	$15-19$	$41-42$	$103-110$
suspect Par.	R	X	b
$\boldsymbol{\lambda}^{N\phi}$	$\begin{bmatrix} \mathbf{70.34} & 44.48 & 40.52 \\ & 9.16 & 16.55 \\ & & 12.75 \end{bmatrix}$	$\begin{bmatrix} 73.02 & 62.63 & 188.18 \\ & 77.07 & 133.76 \\ & & \mathbf{287.63} \end{bmatrix}$	$\begin{bmatrix} 5.25 & 5.30 & 8.87 \\ & \mathbf{16.61} & 1.64 \\ & & 6.29 \end{bmatrix}$
True value	0.020	0.225	0.0359
Err. value	0.026	0.2925	0.04667
Est. value	0.020	0.225	0.0359
Est. Iter	1	2	1

TABLE IV
IDENTIFICATION, AND ESTIMATION OF MULTIPLE PARAMETER ERRORS IN TRANSMISSION LINE: PMU AT ONE END (IEEE 118-BUS SYSTEM)

Erroneous TL Detection	***True Value***	***Erroneous Value***	$\boldsymbol{\lambda}^{N+}$	***Par.***	$\boldsymbol{r}^{N+}$	***Meas.***
	$\begin{bmatrix} 0.18 & 0.072 & 0.072 \\ & 0.18 & 0.072 \\ & & 0.18 \end{bmatrix}$	$\begin{bmatrix} 0.234 & 0.0864 & 0.0864 \\ & 0.234 & 0.0864 \\ & & 0.234 \end{bmatrix}$	1058	X_{3-5}	762.4	$\mathscr{R}\{I_{3-5}\}$
			533.6	X_{1-3}	594.5	$\mathscr{R}\{I_3\}$
			513.4	X_{2-12}	302.5	$\mathscr{R}\{I_{3-12}\}$
Parameter Estimation	$\boldsymbol{\lambda}^{N\phi}$	***Estimated Par.*** (1^{st} ***Iter***)	***Estimated Par.*** (2^{nd} ***Iter***)	***Estimation Error*** (%)		
cycle-1	$\begin{bmatrix} 1343 & 1542 & 549.9 \\ & \mathbf{2203} & 1350 \\ & & 1476 \end{bmatrix}$	$\begin{bmatrix} 0.1916 & 0.0803 & 0.0864 \\ & 0.1782 & 0.0787 \\ & & 0.1854 \end{bmatrix}$	$\begin{bmatrix} 0.1758 & 0.0699 & 0.0684 \\ & 0.1782 & 0.0697 \\ & & 0.1762 \end{bmatrix}$			
cycle-2	$\begin{bmatrix} 2.38 & 2.74 & 2.23 \\ & 5.19 & 3.82 \\ & & \mathbf{5.66} \end{bmatrix}$	$\begin{bmatrix} 0.1762 & 0.0699 & 0.0696 \\ & 0.1789 & 0.0704 \\ & & 0.1774 \end{bmatrix}$	$\begin{bmatrix} 0.1762 & 0.0699 & 0.0696 \\ & 0.1789 & 0.0704 \\ & & 0.1774 \end{bmatrix}$	$\begin{bmatrix} 2.1\% & 2.9\% & 3.3\% \\ & 0.6\% & 2.4\% \\ & & 1.4\% \end{bmatrix}$		

Although all the TLs in *Tests A-C* are transposed, the corrupted parameters deteriorate the symmetry of the TL, and it is not considered a transposed TL anymore. However, the decoupled SE solution is still achievable by employing the compensation method.

For identifying the exact phase of the erroneous parameter, measurements incident to the flagged line are extracted, and their equations are written in the phase domain. For the 6 phase domain parameters, there will be six NLMs where the largest one corresponds to the incorrect phase. Three-phase NLMs ($\boldsymbol{\lambda}^{N\phi}$) are shown in the form of (39) in the third row where the boldface value in $\boldsymbol{\lambda}^{N\phi}$ indicates the largest NLM. True value, erroneous value, and estimated value are reported in the last row. Since the proposed parameter estimation method is iterative, the required number of iterations for each case are also given in Table III. The results show highly accurate estimates of parameters for all cases despite the use of a single PMU at one end of the line.

B. Multiple Parameter Errors in a Transposed TL

This subsection considers a more realistic case of having more than one parameter in error for a three-phase line. This is tested by increasing all the self-reactances of the TL $3-5$ by 30% and all the mutual reactances by 20%. The parameter error detection and estimation results with only one PMU at bus 3 are shown in Table IV.

The top part of Table IV, labeled as *Erroneous TL Detection*, shows the true and erroneous values and the results of parameter and measurement error detection for the positive sequence. For $\boldsymbol{\lambda}^{N+}$ and $\boldsymbol{r}^{N+}$ three largest values along with the associated parameters/measurements are given. As expected, the largest value is related to the reactance X_{3-5}. In the next step, the local sub-network adjacent to TL $3-5$ is considered and the estimation results are shown in the bottom part of Table IV labeled as *Parameter Estimation* where results of the three-phase NLM test are listed under $\boldsymbol{\lambda}^{N\phi}$. In the first cycle, the largest NLM value corresponds to X^{bb}. So, parameters are estimated in two iterations within *cycle-1* by excluding X^{ac} in 1^{st} *Iter* and X^{bb} in 2^{nd} *Iter*, respectively. Following parameter estimation in *cycle-1*, the largest $\boldsymbol{\lambda}^{N\phi}$ is still higher than the threshold. Since the largest NLM is related to X^{cc}, the same process will be repeated with X^{cc} and X^{ab} in *cycle-2*. The algorithm is terminated at the end of the last cycle as $\boldsymbol{\lambda}^{N\phi}$ becomes insignificant. The final estimated parameters are the ones in the last iteration and last cycle. Estimation errors reported at the end of the last cycle are not significant given the severity of six simultaneous correlated errors and a single PMU at one end of the TL.

The same test with the same procedure is repeated by adding another PMU at the other end of the TL, and the results are shown in Table V. Note that error detection results are eliminated in Table V since they are very similar to Table IV although they are not identical. The estimated parameters and the estimation errors

TABLE V
IDENTIFICATION, AND ESTIMATION OF MULTIPLE PARAMETER ERRORS IN TRANSMISSION LINE: PMU AT BOTH ENDS (IEEE 118-BUS SYSTEM)

		$\boldsymbol{\lambda^{N\phi}}$	*Estimated Par.* (1^{st} *Iter)*	*Estimated Par.* (2^{nd} *Iter)*	*Estimation Error* (%)
Parameter Estimation	*cycle-1*	$\begin{bmatrix} 1743 & 1824 & 821.6 \\ & \mathbf{2544} & 1444 \\ & & 1758 \end{bmatrix}$	$\begin{bmatrix} 0.1949 & 0.0811 & 0.0864 \\ & 0.1798 & 0.0791 \\ & & 0.1863 \end{bmatrix}$	$\begin{bmatrix} 0.1794 & 0.0717 & 0.0716 \\ & 0.1798 & 0.0718 \\ & & 0.1795 \end{bmatrix}$	
	cycle-2	$\begin{bmatrix} 1.81 & 2.25 & 0.69 \\ & \mathbf{3.35} & 2.57 \\ & & 2.82 \end{bmatrix}$	$\begin{bmatrix} 0.1795 & 0.0718 & 0.0716 \\ & 0.1798 & 0.0718 \\ & & 0.1797 \end{bmatrix}$	$\begin{bmatrix} 0.1795 & 0.0718 & 0.0716 \\ & 0.1798 & 0.0718 \\ & & 0.1797 \end{bmatrix}$	$\begin{bmatrix} 0.28\% & 0.27\% & 0.55\% \\ & 0.11\% & 0.25\% \\ & & 0.17\% \end{bmatrix}$

TABLE VI
IDENTIFICATION, AND ESTIMATION OF MULTIPLE PARAMETER ERRORS IN UNTRANSPOSED TRANSMISSION LINE: PMU AT ONE END (IEEE 118-BUS SYSTEM)

		True Value	*Erroneous Value*	$\boldsymbol{\lambda^{N+}}$	*Par.*	$\boldsymbol{r^{N+}}$	*Meas.*
Erroneous TL Detection		$\begin{bmatrix} 0.18 & 0.0713 & 0.0739 \\ & 0.1885 & 0.0773 \\ & & 0.1843 \end{bmatrix}$	$\begin{bmatrix} 0.216 & 0.0784 & 0.0813 \\ & 0.2262 & 0.0850 \\ & & 0.2211 \end{bmatrix}$	808.7	X_{3-5}	581.5	$\mathscr{R}\{I_{3-5}\}$
				417	X_{1-3}	442.7	$\mathscr{R}\{I_3\}$
				339.7	X_{2-12}	235.2	$\mathscr{R}\{I_{3-12}\}$
		$\boldsymbol{\lambda^{N\phi}}$	*Estimated Par.* (1^{st} *Iter)*	*Estimated Par.* (2^{nd} *Iter)*	*Estimation Error* (%)		
Parameter Estimation	*cycle-1*	$\begin{bmatrix} 973 & 1058 & 460.7 \\ & \mathbf{1608} & 1045 \\ & & 1128 \end{bmatrix}$	$\begin{bmatrix} 0.1856 & 0.0752 & 0.0813 \\ & 0.1877 & 0.0801 \\ & & 0.1866 \end{bmatrix}$	$\begin{bmatrix} 0.178 & 0.0704 & 0.0724 \\ & 0.1877 & 0.0766 \\ & & 0.1829 \end{bmatrix}$	$\begin{bmatrix} 1.1\% & 1.2\% & 2\% \\ & 0.4\% & 0.9\% \\ & & 0.7\% \end{bmatrix}$		

TABLE VII
IDENTIFICATION, AND ESTIMATION OF MULTIPLE PARAMETER ERRORS IN MULTIPLE TRANSMISSION LINES (IEEE 118-BUS SYSTEM)

	Erroneous TL Detection				*Parameter Estimation*	
	$\boldsymbol{\lambda^{N+}}$	*Par.*	*True Value*	*Erroneous Value*	$\boldsymbol{\lambda^{N\phi}}$	*Estimated Par.*
1	373.4	X_{15-33}	$\begin{bmatrix} 0.2073 & 0.0829 & 0.0829 \\ & 0.2073 & 0.0829 \\ & & 0.2073 \end{bmatrix}$	$\begin{bmatrix} 0.2487 & 0.0911 & 0.0911 \\ & 0.2487 & 0.0911 \\ & & 0.2487 \end{bmatrix}$	$\begin{bmatrix} \mathbf{243.6} & 44.1 & 11.8 \\ & 26.4 & 20.3 \\ & & 15.3 \end{bmatrix}$	$\begin{bmatrix} 0.2082 & 0.0828 & 0.0829 \\ & 0.2062 & 0.0844 \\ & & 0.2107 \end{bmatrix}$
2	312.1	X_{15-19}	$\begin{bmatrix} 0.0657 & 0.0263 & 0.0263 \\ & 0.0657 & 0.0263 \\ & & 0.0657 \end{bmatrix}$	$\begin{bmatrix} 0.0788 & 0.0289 & 0.0289 \\ & 0.0788 & 0.0289 \\ & & 0.0788 \end{bmatrix}$	$\begin{bmatrix} \mathbf{321} & 215.2 & 187.7 \\ & 304.1 & 162.2 \\ & & 280.9 \end{bmatrix}$	$\begin{bmatrix} 0.0659 & 0.0265 & 0.0265 \\ & 0.0658 & 0.0265 \\ & & 0.0659 \end{bmatrix}$

are both improved in comparison with the case of single-end PMU due to the increased measurement redundancy.

C. Multiple Parameter Errors in an Untransposed TL

Parameter errors in untransposed TLs can also be handled by using the proposed method. Since all the TLs in the IEEE-118 bus system are transposed, TL $3-5$ is replaced by an untransposed TL. Then self reactances (all phases) are increased by 20%, and the mutual reactances (all phases) are increased by 10%. Results of parameter error detection and estimation are shown in Table VI considering that only one PMU is installed at bus 3 and no PMU at bus 5. It is worth noting that the decoupled formulation can still be used thanks to the decoupled SE method introduced in Section II.C. As evident from Table VI, following the identification of the error, only one cycle is needed to estimate the correct parameters of the TL, validating the suitability of the method in the presence of both untransposed as well as transposed TLs.

D. Multiple Parameter Errors in Multiple TLs

In this subsection, a more challenging case is considered where the parameters of two TLs incident to the same bus are erroneous. Self and mutual reactances of both lines $15-33$ and $15-19$ are increased by 20% and 10% respectively. Results of error detection / estimation are shown in Table VII.

As evident in Table VII, in the first cycle, the parameter X_{15-33} is identified as erroneous having its NLM as the largest among all the network parameters in the positive sequence network. After correcting full three-phase X_{15-33}, the next cycle detects X_{15-19} as the erroneous parameter and it is also corrected. Despite the proximity of the parameter errors they are successfully handled in this case. Note that the same rule is applied for choosing the local sub-network since the accuracy of the estimated parameters is acceptable. However, after detecting the second suspect TL and considering their close proximity, it is possible to expand the local sub-network by considering the one-tier out buses from all three buses and further refine the parameters by repeating the identification cycle for the expanded sub-network.

It must be noted that parameter errors may not always be identifiable in rare cases when they are strongly interacting and conforming since the method relies on detection and correction cycles of a single error at a time. This is similar to the inherent limitation of the largest normalized residual test for bad data due to the cyclic detection and correction of errors one at a time.

TABLE VIII
IDENTIFICATION, AND ESTIMATION OF MULTIPLE PARAMETER ERRORS IN TRANSMISSION LINE (LARGE UTILITY SYSTEM)

Erroneous TL Detection	***True Value***			***Erroneous Value***			$\boldsymbol{\lambda}^{N+}$ ***Par.***	$\boldsymbol{r}^{N+}$ ***Meas.***
	$\begin{bmatrix} 0.2933 & 0.1173 & 0.1173 \\ & 0.2933 & 0.1173 \\ & & 0.2933 \end{bmatrix}$			$\begin{bmatrix} 0.3519 & 0.129 & 0.129 \\ & 0.3519 & 0.129 \\ & & 0.3519 \end{bmatrix}$			$\begin{matrix} 245.2 \\ 232.9 \\ 227.1 \end{matrix}$ $\begin{matrix} X_{1587-1591} \\ X_{1591-1308} \\ X_{1308-1516} \end{matrix}$	$\begin{matrix} 139.6 \\ 139.5 \\ 94.2 \end{matrix}$ $\begin{matrix} \mathscr{R}\{I_{1587-1591}\} \\ \mathscr{I}\{I_{1587-1591}\} \\ \mathscr{R}\{I_{1587-1308}\} \end{matrix}$
Parameter Estimation	$\boldsymbol{\lambda}^{N\phi}$			***Estimated Par.*** (1^{st} ***Iter***)			***Estimated Par.*** (2^{nd} ***Iter***)	***Estimation Error*** (%)
cycle-1	$\begin{bmatrix} 75.2 & 69.1 & 7.5 \\ & 102.3 & 166.4 \\ & & \mathbf{289.2} \end{bmatrix}$			$\begin{bmatrix} 0.2993 & 0.1190 & 0.1176 \\ & 0.3136 & 0.1174 \\ & & 0.2934 \end{bmatrix}$			$\begin{bmatrix} 0.2943 & 0.1181 & 0.1170 \\ & 0.2954 & 0.1169 \\ & & 0.2934 \end{bmatrix}$	$\begin{bmatrix} 0.3\% & 0.7\% & 0.2\% \\ & 0.7\% & 0.3\% \\ & & 0.03\% \end{bmatrix}$

TABLE IX
IDENTIFICATION, AND ESTIMATION OF SINGLE PARAMETER ERROR: WITH GAUSSIAN NOISE (IEEE 118-BUS SYSTEM)

	Test A	***Test B***
$\boldsymbol{r}^{N0}$ $\boldsymbol{r}^{N+}$	10.64 27.70	20.49 102.9
$\boldsymbol{\lambda}^{N0}$ $\boldsymbol{\lambda}^{N+}$	13.25 **34.71**	34.17 **125.81**
suspect TL	$15-19$	$41-42$
suspect Par.	R	X
$\boldsymbol{\lambda}^{N\phi}$	$\begin{bmatrix} \mathbf{69.55} & 44.56 & 38.90 \\ & 10.64 & 15.13 \\ & & 12.49 \end{bmatrix}$	$\begin{bmatrix} 74.40 & 61.55 & 188.16 \\ & 76.67 & 132.13 \\ & & \mathbf{286.15} \end{bmatrix}$
True value	0.020	0.225
Err. value	0.026	0.2925
Est. value	0.0198	0.2256

E. Scalability of the Proposed Method

In this section, a large 3474-bus utility system with 4644 branches is studied to verify the scalability of the proposed method. Self and mutual reactances of the TL $1587-1591$ are increased by 20% and 10% respectively, where $\mathcal{N}_{1587} = \{2263, 1591\}$ and $\mathcal{N}_{1591} = \{1308, 1595, 1587\}$. Results of parameter error detection / estimation are shown in Table VIII. Explanations similar to those in previous subsections also hold true for Table VIII.

F. Impact of Gaussian Noise on the Proposed Method

So far, the PMU measurements are considered to be noise-free in all the above cases. In this part, *Tests A* and *B* described in Section V-A are repeated by adding Gaussian noise with zero mean and 10^{-3} standard deviation to all the measurements and the results are shown in Table IX. Although the NR and NLM values are not the same as those given in Table III, suspect TL is correctly detected. As expected, the estimation errors are slightly larger for both tests due to the presence of measurement noise but still in the same order of magnitude as the standard deviations of measurement errors.

VI. CONCLUSION

This paper presents an algorithm for parameter error detection, identification, and estimation of three-phase transmission lines in a large power grid. The distinguishing features of the approach are its handling of both transposed and untransposed lines, its use of modal-decoupled PMU-based linear estimator with compensation, and its use of a limited number of PMUs, which are placed via a new PMU placement algorithm. The presented method is expected to be useful in correcting database errors in detailed three-phase network models and improving the accuracy and reliability of the network applications that rely on that database.

REFERENCES

[1] C. Hansen and A. Debs, "Power system state estimation using three-phase models," *IEEE Trans. Power Syst.*, vol. 10, no. 2, pp. 818–824, May 1995.

[2] Y. Liao and M. Kezunovic, "Online optimal transmission line parameter estimation for relaying applications," *IEEE Trans. Power Del.*, vol. 24, no. 1, pp. 96–102, Jan. 2009.

[3] M. Kato, T. Hisakado, H. Takani, H. Umezaki, and K. Sekiguchi, "Live line measurement of untransposed three phase transmission line parameters for relay settings," in *Proc. IEEE Power Energy Soc. Gen. Meeting*, Jul. 2010, pp. 1–8.

[4] J. De La Ree, V. Centeno, J. S. Thorp, and A. G. Phadke, "Synchronized phasor measurement applications in power systems," *IEEE Trans. Smart Grid*, vol. 1, no. 1, pp. 20–27, Jun. 2010.

[5] G. Korres and N. Manousakis, "State estimation and observability analysis for phasor measurement unit measured systems," *IET Gener., Transmiss. Distrib.*, vol. 6, no. 9, pp. 902–913, Sep. 2012.

[6] S. Sarri, L. Zanni, M. Popovic, J.-Y. Le Boudec, and M. Paolone, "Performance assessment of linear state estimators using synchrophasor measurements," *IEEE Trans. Instrum. Meas.*, vol. 65, no. 3, pp. 535–548, Mar. 2016.

[7] L. Zanni *et al.*, "PMU-based linear state estimation of Lausanne sub-transmission network: Experimental validation," *Electric Power Syst. Res.*, vol. 189, pp. 1–7, Dec. 2020.

[8] K. D. Jones, J. S. Thorp, and R. M. Gardner, "Three-phase linear state estimation using phasor measurements," in *Proc. IEEE Power Energy Soc. Gen. Meeting*, Jul. 2013, pp. 1–5.

[9] A. G. Phadke *et al.*, "Synchrophasor based tracking three-phase state estimator and it's applications," Blacksburg, VA, USA: Virginia Tech, Tech. Rep. DOE 2010, *Transmission Reliability Program Peer Review*, Oct. 2013. [Online]. Available: https://www.osti.gov/biblio/1128928

[10] D. Roop and K. D. Jones, "Synchrophasors at dominion energy," Sep. 2020. [Online]. Available: https://www.naspi.org/sites/default/files/2020-10/20200930_naspi_webinar.pdf

[11] M. Göl and A. Abur, "A robust PMU based three-phase state estimator using modal decoupling," *IEEE Trans. Power Syst.*, vol. 29, no. 5, pp. 2292–2299, Sep. 2014.

[12] R. Khalili and A. Abur, "PMU-based decoupled state estimation for unsymmetrical power systems," *IEEE Trans. Power Syst.*, vol. 36, no. 6, pp. 5359–5368, Nov. 2021, doi: 10.1109/TPWRS.2021.3069738.

[13] M. Asprou and E. Kyriakides, "Identification and estimation of erroneous transmission line parameters using PMU measurements," *IEEE Trans. Power Del.*, vol. 32, no. 6, pp. 2510–2519, Dec. 2017.

[14] D. Shi, D. J. Tylavsky, N. Logic, and K. M. Koellner, "Identification of short transmission-line parameters from synchrophasor measurements," in *Proc. 40th North Amer. Power Symp.*, Sep. 2008, pp. 1–8.

[15] K. Dasgupta and S. Soman, "Line parameter estimation using phasor measurements by the total least squares approach," in *Proc. IEEE Power Energy Soc. Gen. Meeting*, Jul. 2013, pp. 1–5.

[16] D. Ritzmann, P. S. Wright, W. Holderbaum, and B. Potter, "A method for accurate transmission line impedance parameter estimation," *IEEE Trans. Instrum. Meas.*, vol. 65, no. 10, pp. 2204–2213, Oct. 2016.

[17] P. A. Pegoraro, K. Brady, P. Castello, C. Muscas, and A. von Meier, "Line impedance estimation based on synchrophasor measurements for power distribution systems," *IEEE Trans. Instrum. Meas.*, vol. 68, no. 4, pp. 1002–1013, Apr. 2019.
[18] D. Shi, D. J. Tylavsky, K. M. Koellner, N. Logic, and D. E. Wheeler, "Transmission line parameter identification using PMU measurements," *Eur. Trans. Elect. Power*, vol. 21, no. 4, pp. 1574–1588, May 2011.
[19] V. Milojević, S. Čalija, G. Rietveld, M. V. Ačanski, and D. Colangelo, "Utilization of PMU measurements for three-phase line parameter estimation in power systems," *IEEE Trans. Power Syst.*, vol. 67, no. 10, pp. 2453–2462, Oct. 2018.
[20] A. Wehenkel, A. Mukhopadhyay, J.-Y. Le Boudec, and M. Paolone, "Parameter estimation of three-phase untransposed short transmission lines from synchrophasor measurements," *IEEE Trans. Instrum. Meas.*, vol. 69, no. 9, pp. 6143–6154, Sep. 2020.
[21] R. Puddu, K. Brady, C. Muscas, P. A. Pegoraro, and A. Von Meier, "PMU-based technique for the estimation of line parameters in three-phase electric distribution grids," in *Proc. IEEE Int. Workshop Appl. Meas. Power Syst.*, Sep. 2018, pp. 1–5.
[22] Z. Wu, L. T. Zora, and A. G. Phadke, "Simultaneous transmission line parameter and PMU measurement calibration," in *Proc. IEEE Power Energy Soc. Gen. Meeting*, Jul. 2015, pp. 1–5.
[23] P. Ren, H. Lev-Ari, and A. Abur, "Tracking three-phase untransposed transmission line parameters using synchronized measurements," *IEEE Trans. Power Syst.*, vol. 33, no. 4, pp. 4155–4163, Jul. 2018.
[24] S. Gajare, A. K. Pradhan, and V. Terzija, "A method for accurate parameter estimation of series compensated transmission lines using synchronized data," *IEEE Trans. Power Syst.*, vol. 32, no. 6, pp. 4843–4850, Nov. 2017.
[25] V. Quintana and T. Van Cutsem, "Power system network parameter estimation," *Optim. Control Appl. Methods*, vol. 9, no. 3, pp. 303–323, 1988.
[26] T. Van Cutsem and V. Quintana, "Network parameter estimation using online data with application to transformer tap position estimation," *IEE Proc. (Gen. Transmiss. Distrib.)*, vol. 135, no. 1, pp. 31–40, Jan. 1988.
[27] W.-H. Liu, F. F. Wu, and S.-M. Lun, "Estimation of parameter errors from measurement residuals in state estimation (power systems)," *IEEE Trans. Power Syst.*, vol. 7, no. 1, pp. 81–89, Feb. 1992.
[28] I. W. Slutsker, S. Mokhtari, and K. A. Clements, "Real time recursive parameter estimation in energy management systems," *IEEE Trans. Power Syst.*, vol. 11, no. 3, pp. 1393–1399, Aug. 1996.
[29] W.-H. Liu and S.-L. Lim, "Parameter error identification and estimation in power system state estimation," *IEEE Trans. Power Syst.*, vol. 10, no. 1, pp. 200–209, Feb. 1995.
[30] P. Zarco and A. Gomez, "Off-line determination of network parameters in state estimation," in *Proc. 20th Power Syst. Comput. Conf.*, 1996, pp. 1207–1213.
[31] Y. Lin and A. Abur, "A new framework for detection and identification of network parameter errors," *IEEE Trans. Smart Grid*, vol. 9, no. 3, pp. 1698–1706, May 2018.
[32] Y. Lin and A. Abur, "Strategic use of synchronized phasor measurements to improve network parameter error detection," *IEEE Trans. Smart Grid*, vol. 9, no. 5, pp. 5281–5290, Sep. 2018.
[33] L. Zhang and A. Abur, "Strategic placement of phasor measurements for parameter error identification," *IEEE Trans. Power Syst.*, vol. 28, no. 1, pp. 393–400, Feb. 2013.
[34] R. Khalili and A. Abur, "Detection of errors in three-phase line models using synchronized phasor measurements," in *Porc. IEEE PES Innov. Smart Grid Technol. Conf. Eur.*, Oct. 2020, pp. 1131–1135.
[35] B. Xu and A. Abur, "Observability analysis and measurement placement for systems with PMUs," in *Proc. IEEE PES Power Syst. Conf. Expo.*, Oct. 2004, pp. 943–946.
[36] M. Korkali and A. Abur, "Placement of PMUs with channel limits," in *Proc. IEEE Power Energy Soc. Gen. Meeting*, Jul. 2009, pp. 1–4.
[37] P. Zarco and A. G. Exposito, "Power system parameter estimation: A survey," *IEEE Trans. Power Syst.*, vol. 15, no. 1, pp. 216–222, Feb. 2000.

Ramtin Khalili (Student Member, IEEE) received the B.S. degree from the K.N.Toosi University of Technology and the M.S. degree from the Amirkabir University of Technology, Tehran, Iran. He is currently working toward the Ph.D. degree in power system with Northeastern University, Boston, MA, USA. His research interests include power system modeling, state estimation, and control.

Ali Abur (Fellow, IEEE) received the B.S. degree in electrical engineering from Orta Dogu TeknikUniversitesi, Ankara, Turkey, and the M.S. and Ph.D. degrees from The Ohio State University, Columbus, OH, USA. He is currently a Professor with the Electrical and Computer Engineering Department, Northeastern University, Boston, MA, USA.